

EMERGENCY MICROPILE REPAIR OF THE BIRMINGHAM BRIDGE

Terence P. Holman, Ph.D., P.E.¹ and Scott A. Stonecheck, P.E.²

ABSTRACT: On February 8, 2008, a steel rocker bearing failure at Pier 10 of the Birmingham Bridge caused an 200 mm drop between two adjacent spans. This emergency situation forced PennDOT District 11-0 personnel to retain a general contractor to immediately shore up the steel girders of the spans to prevent further collapse. This case history describes the implementation of an aggressive micropile retrofit solution, developed by the specialty contractor and design consultant, to re-support the failed Pier 10 S and ultimately Pier 10N. The proposed retrofit incorporated the use of thirty three micropiles drilled through the existing concrete pile cap and between steel H-piles in a 4.9 m wide space between the existing false-work towers. An additional twenty two micropiles were placed around the existing Pier 10N crash wall to bolster the structural capacity of the pier. Typical micropile lengths were 25.6 m.

This paper presents detailed information on these bridge substructure retrofits and the implementation of a micropile solution for these emergency repairs. Load and Resistance Factor design methods were used to generate an efficient micropile section to be advanced deep into the subsurface to bypass the weak units thought to be responsible for the Pier 10S failure. Two load tests were conducted on the same test pile; one as part of the Pier 10S design verification and one to examine the possibilities for greater design loadings for adjacent Pier 10N. The results of these cyclic tests were used to make a detailed assessment of pseudo-elastic behavior of the piles, including the decomposition of elastic and plastic behaviors and mobilization of load transfer. Estimated bond stresses at pre-failure loads in the rock socket were less than assumed in design, primarily because the cased length of the pile, approximately 21 m long, transferred nearly 1,000 kN of load to the overburden soils and weak rock.

INTRODUCTION

On 8 February 2008, two land spans of the Birmingham Bridge settled up to 200 mm in the overnight hours, leading the Pennsylvania Department of Transportation (PennDOT) to close the bridge. This tied-arch bridge, built in 1976, is a major link in the Pittsburgh transportation system, serving as a heavily traveled crossing of the Monongahela River. An initial inspection of the bridge revealed that the steel rocker bearings at Pier 10S had over-rotated and failed, causing the steel girders to drop onto the pier cap (Figure 1). In addition, the top of Pier 10S was horizontally displaced 230 mm towards the river and cracks of up to 6 mm were observed at the base of the columns, indicating significant bending moments and rotation about the foundation substructure. The cause of the performance failure was unknown, but due to the critical role of the bridge in the regional transportation system, the bridge needed to be made serviceable and reopened.

Under an emergency contract, PennDOT engaged a local heavy-highway general contractor and consulting engineer to stabilize the failed southbound spans around Pier 10S and begin development of a remedial program to allow reopening of the bridge. A system of lattice shoring towers were used to support the steel girders formerly bearing on top of Pier 10S, with the towers bearing on timbers mats placed directly on-grade. The dead loads of the adjoining

¹ Senior Engineer, MORETRENCH, 100 Stickle Avenue, Rockaway, NJ 07866, tholman@mtac.com

² Area Manager, MORETRENCH, 144 Dexter Drive, Monroeville, PA 15146, sstonecheck@mtac.com

spans to Pier 10S were transferred to the shoring towers to allow the bridge to be re-opened to limited vehicular traffic.



Figure 1. Failed rocker bearing at Pier 10S (adapted from Splitstone et al, 2010)

The failure investigation for Pier 10S centered on performance issues with the foundation. As part of the failure investigation, the geotechnical consultant performed an evaluation of the damaged pier below the fallen spans, including the as-built tip locations. Induction Field (IF) testing was performed on two of the original driven piles. This nondestructive test method, detailed in Olsen et al (1998), involves sensing a change in the magnetic field between the deep foundation and a nearby sensing coil lowered into a cased borehole, was used to estimate the as-built pile lengths. IF testing indicated that the existing piles, driven prior to 1976, were above the top of hard rock elevations estimated from the original contract test boring logs. The investigation concluded that a thin layer of hard rock had prevented the piles from being driven through a soft rock layer known locally as the Pittsburgh Redbed into the underlying competent rock layer 7.5 to 9 m lower. Refer to Figure 2 for an illustration of the typical subsurface conditions beneath the project site. The exact cause of the sudden pile group failure and rotation of the pier is still unknown, but calculations indicated that the theoretical margin of safety for service loads was less than one, implying that the bearing area at the base of the pile cap may have been providing significant foundation capacity.

DEVELOPMENT OF CONSTRUCTIBLE RETROFIT SOLUTIONS

Long-term remediation solutions for the Pier 10S foundation involved advancing new foundations into the underlying rock mass. The general contractor consulted with the specialty geotechnical contractor's engineering staff to assist in development of retrofit solutions. A meeting was held involving PennDOT engineering and construction staff to discuss the possible solutions. Any constructible retrofit would have to consider the working area limitations caused by the use of shoring towers to support the spans adjacent to Pier 10S. The clear distance between the shoring towers was 4.9 m and the headroom from existing grade to the underside of the girders above was 17 m. The bottom of the existing H-pile supported cap was situated

3.7 m below grade. The adjacent shoring towers, under load from the bridge above, had induced an elevated level of vertical and horizontal stress in the ground surrounding the existing substructure, making a deep excavation to remove the pile cap impractical without potentially destabilizing the shoring towers. The geotechnical contractor, in recognition of these issues, recommended the use of a micropile retrofit system for Pier 10S rather than driven H-piles, drilled shaft foundations, or grouting for ground improvement. Micropiles have a track record of successful installation in constrained space conditions, significant load-carrying capacity at small diameters, and readily available tooling to advance pile casings through obstructions and buried structures.

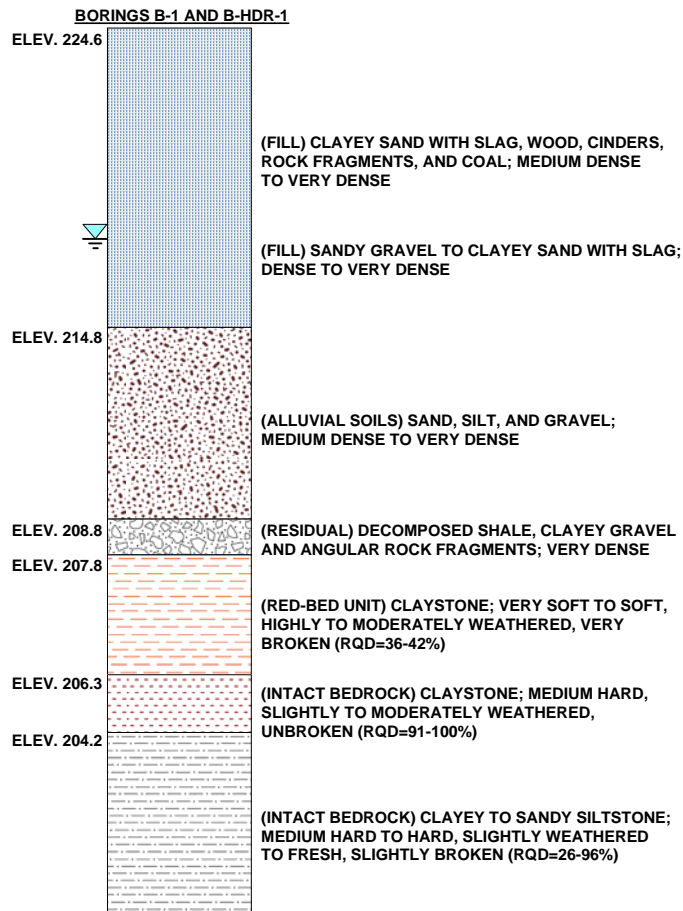


Figure 2. Detailed subsurface conditions at Pier 10S, test borings B-1 and B-HDR-1.

DESIGN OF MICROPILE RETROFIT FOR THE BIRMINGHAM BRIDGE

PIER 10S

The design for the micropile retrofit was developed by PennDOT's consultant with the active participation of the specialty contractor. In order to provide an effective remedial design, the specialty contractor focused on developing a solution in which the existing substructure and 48 HP250x63 group could remain in place while a new micropile group was constructed around them. This requirement stemmed from the fact that any excavation in between the shoring towers would be likely to induce vertical and horizontal movements, leading to destabilization of

the shoring. The specialty contractor proposed that the micropile foundation should be constructed by drilling new piles through the buried foundation, in between the existing H-piles. In discussions this construction method was deemed feasible from a constructability standpoint and because the lateral loading in the substructure was not substantial. This would allow a near-surface pile group to be installed and a cap constructed with very little excavation.

The design of the micropile retrofit and new substructure was performed in accordance with AASHTO and PennDOT Load and Resistance Factor (LRFD) design procedures. All substructure design was conducted by the general contractor's design consultant. Multiple Service and Strength Limit load states were examined in accordance with PennDOT procedures. Table 1 summarizes the range of Strength and Service loads on the entire substructure, not including an estimated 1.52 m thick cap dead load.

Table 1. Summary of total loads on Pier 10S not including pile cap dead load

	Strength III and I		Service I	
	Minimum	Maximum	Minimum	Maximum
Axial Load (MN)	19.8	32.5	16.7	21.7
Transverse Moment (MN-m)	0.8	7.9	1.2	2.6
Longitudinal Moment (MN-m)	0.4	8.4	2.0	5.1
Transverse Shear (kN)	89.0	996.4	160.1	355.9
Longitudinal Shear (kN)	35.6	391.4	89.0	177.9

The dimensions of the original pile cap were 21 m by 4.57 m. The geotechnical specialty contractor, based on experience in similar rock formations, suggested that in order to limit the micropile group geometry that a relatively high Strength Limit capacity was possible and should be utilized. The individual micropile design loads on the new substructure were estimated as shown in Table 2 below and based on the use of 33 micropiles for support of the retrofitted pier. The maximum axial design loads and required resistances were based on Strength I loading, while tension and lateral loads were a result of Strength III load effects. For ease in conducting axial compression load tests in accordance with PennDOT and ASTM standards, the working (allowable) axial compression load was taken as 890 kN, reflecting an average load factor of 1.52.

Table 2. Summary of individual micropile design loads

	Static Load	Load Group
Axial Compression Resistance (kN)	1355	Strength I
Max. Design Pile Axial Load (kN)	1196	
Axial Uplift Resistance (kN)	0	Strength III
Max. Design Axial Uplift Load (kN)	7	
Pile Lateral Resistance (kN)	33	Strength III
Max. Design Pile Lateral Load (kN)	33	

The emergency repair nature of this project necessitated that the micropile size be selected based on readily available pipe casing and reinforcing bar sizes. The preliminary meetings between project team members and consultation with mill secondary casing suppliers had resulted in the selection of 194 mm OD casing with a 12.7 mm or 10.2 mm wall thickness. This flush-joint casing was available in minimum yield strength of 552 MPa. Based on the casing

characteristics, the pile geometry was set to allow the structural and geotechnical design of the micropiles to be completed. Figure 3 illustrates a vertical section through the design micropile section. Because of the use of high strength flush joint casing with $F_y=552$ MPa, no centralized reinforcing bar was required for the cased length of the pile except for a 1.83 m development length. For the rock socket, assumed to be 152 mm in minimum diameter, the reinforcing bar was required to be a 63 mm Grade 552 (ASTM A615) threadbar assuming that the design compressive strength f'_c of the neat cement grout was 27.6 MPa. PennDOT's "Micropile LRFD Specification" includes equations and resistance factors for structural and geotechnical Strength Limit resistance of the cased portion and rock socket (uncased length) and is the design specification used for this project. For the micropile cased and uncased zone described above and used in the preliminary design, the Strength Limit resistances of the micropile segments are:

Cased Length

$$R_{cc} = \phi_{cc} R_n = \phi_{cc} [0.85 f'_c A_g + F_y A_c]$$

$$R_{cc} = 0.65 [0.85(27.6 \text{MPa})(0.0192 \text{m}^2) + (552 \text{MPa})(0.00723 \text{m}^2)] \quad (\text{Eq. 1})$$

$$R_{cc} = 2.89 \text{MN} = 2,890 \text{kN} \gg 1,196 \text{kN}$$

Rock Socket

$$R_{cu} = \phi_{cu} R_n = \phi_{cu} [0.85 f'_c A_g + F_{yb} A_b]$$

$$R_{cc} = 0.65 [0.85(27.6 \text{MPa})(0.0151 \text{m}^2) + (552 \text{MPa})(0.00317 \text{m}^2)] \quad (\text{Eq. 2})$$

$$R_{cc} = 1.37 \text{MN} = 1,370 \text{kN} > 1,196 \text{kN}$$

For both the cased length and rock socket, the assumed geometries and materials provided a Service Limit capacity greater than the maximum factored load on an individual pile. For comparison with the Federal Highway Administration Allowable Stress Design methodology as described in Sabatini et al (2005), the operative design (working) structural capacity of the rock socket was 941 kN, indicating that under an accepted, alternate design methodology the pile structural design was also sufficient.

For economy and in consideration of the fact that the tension loads on the piles were negligible, the centralized reinforcing bar was only used in the rock socket and for a development length into the bottom of the casing. The design consultant selected a development length of 1.83 m, approximately 30 bar diameters. This development length is consistent with common practice for compression-only loaded micropiles and does not necessarily comply with the typical American Concrete Institute (ACI) 318-05 practices. In ACI, bar development lengths are commonly designed for tension embedment and typically fall within the range of 40 to 50 bar diameters for this type of loading.

The geotechnical design of the micropile, in this case, centered around determining the required rock socket length to support the entire axial compression Strength Limit load of 1,196 kN. Conservatively, no side resistance in the overburden fill material (consisting of gravelly sands and gravels, slag, brick and wood fragments, and coal) was assumed to contribute to the overall nominal micropile axial capacity. Following the forensic investigation to determine the cause of failure for Pier 10S, the additional test borings had determined that a layer of weak sedimentary claystone known as the "Pittsburgh Redbed" had caused premature driving refusal of the original H-piles. As shown in Figure 2, this layer was estimated to exist at Elev. 207.8, approximately 16.5 m below the working grade. The sound, moderately broken, medium hard

to hard competent siltstone, claystone, and sandstone bedrock found beginning at Elev. 203 was identified as the rock mass in which the bond zone of the micropiles was to be developed. This layer has NX-sized core recoveries approaching or equaling 100% and Rock Quality Designations greater than 50%. Based on preliminary ultimate grout-to-ground bond (α_b) values found in Sabatini et al (2005), ultimate bond stresses in these rock types would be expected to range from 517 to 1380 kPa. Similar values can be found in Hanna (1982) for rock types around the world. For design, an ultimate bond stress α_b of 1,034 kPa was chosen for use with PennDOT's LRFD design specification. This value, coupled with an LRFD resistance factor ϕ_s of 0.60 (for presumptive values of α_b) to 0.80 (if static load testing is to be used), results in a factored Strength Limit geotechnical resistance for the rock socket of

$$Q_r = \phi_s Q_s = \phi_s \pi d_b \alpha_b L_b = (0.60 \text{ to } 0.80)(\pi)(0.152 \text{ m})(1,034 \text{ kPa})(L_b) \quad (\text{Eq. 3})$$

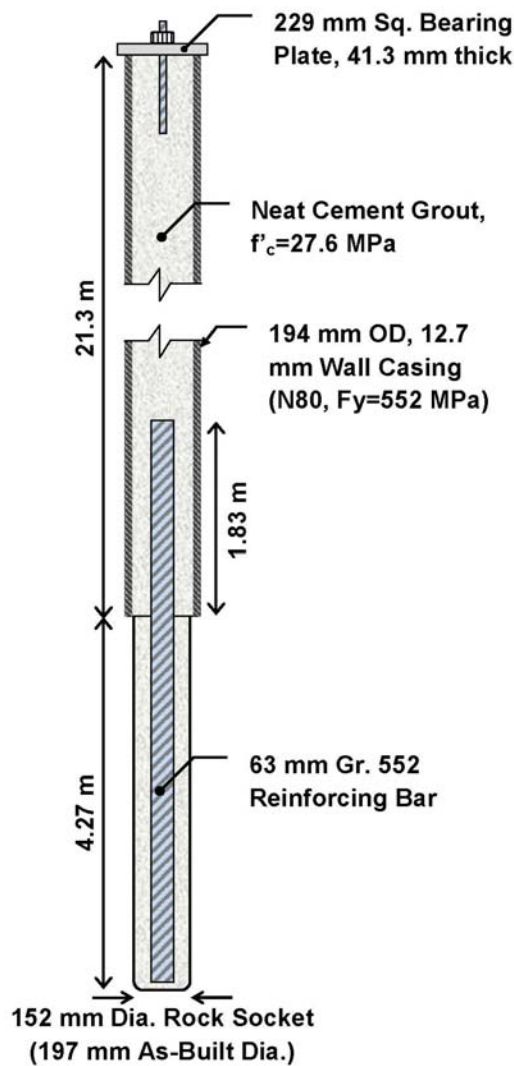


Figure 3. Rock-socketed micropile details

For a required axial Strength Limit load of 1,196 kN, the required rock socket length would vary from 3.0 to 4.0 m. If sizing the socket based on the largest factored load, the Strength I axial compression resistance 1,355 kN, the rock socket length L_b would vary from 3.4 to 4.6 m. For design and construction purposes, the consultant specified a design bond length of 4.27 m. Relative to the rock socket design (working) structural capacity of 941 kN, this bond length results in a uniform average load transfer rate of 440 kN/m and a working bond stress of 920 kPa for a mobilized bond length equal 2.13 m, half of the installed length of 4.27 m.

PIER 10N

In the process of inspecting the Birmingham Bridge after the failure at Pier 10S, it was discovered that the rocker bearings at the adjacent Pier 10N had also suffered over-rotation. No damage was observed to the pier columns or other parts of the substructure, but PennDOT decided that foundation retrofit was required to prevent damage similar to that which has occurred at Pier 10S. Similar non-destructive testing as was employed at Pier 10S was used to confirm that the driven H-pile tip elevations were also sitting in the Red-Bed claystone. Solutions other than micropile retrofit were considered, including grouting for soil and weak rock stabilization, but these methods could not provide guaranteed support. Because the specialty contractor was still on-site completing the Pier 10S piles, it was

determined that micropile retrofitting was the most cost-effective solution. However, the presence of a large crash wall for Pier 10N prevented an equal number of piles from being installed as for Pier 10S, and necessitated the use of a higher pile capacity.

Following the successful performance of the test pile at Pier 10S, PennDOT, its consultants, and the general and specialty contractor felt that the 194 mm OD micropiles could sustain a larger load for the same cased section, same rock socket length and diameter, but a larger centralized reinforcing bar. The size of the reinforcing bar was increased to an 89 mm Grade 552 to provide the required factored structural resistance. An additional load test was specified and was to be run on the same test pile for Pier 10S to prove that an elevated load could be carried. The design consultant specified that the new design (working) load was to be 1,280 kN, related to a Strength Limit Resistance of 1,690 kN. Based on these LRFD design criteria, a total of 22 micropiles were specified and installed in the same manner as for Pier 10S.

LOAD TESTING PROGRAM

While the general contractor was demolishing the pier columns and crash wall down to subgrade at Pier 10S, the specialty geotechnical contractor was preparing to perform a static axial compression load test on a sacrificial micropile. A test pile was installed using 194 mm OD casing size with 10.9 mm wall thickness and yield strength over 850 MPa. A concentric overburden drilling system was employed to advance the test pile casing through the fill soils, obstructions, and the soft Redbed claystones to reach the competent rock below. This type of rotary percussion drilling system, as shown in Figure 4, allows the pipe casing to be carried down through overburden soils, cobbles and boulders, and soft rock to seat the casing bit into rock. After reaching the rock surface, the down the hole hammer was advanced below the bottom of the casing to drill the rock socket. For the casing pipe size used in this project, the maximum diameter of the specialized percussion bit was 197 mm, larger than the minimum rock socket diameter of 152 mm specified by the consultant. Sound rock was encountered at Elev. 201.8, where the casing was stopped, followed by construction of a 4.9 m long rock socket. The overall cased length of the test pile was 22.8 m. The test pile was grouted under tremie head followed by a curing period during which time the load test reaction frame was installed and setup.

The reaction system for the specified cyclic compression load test to 2.0 times the design (working) load of 890 kN, equal to 1,780 kN, consisted of two tension reaction anchors and a double wide-flange test beam. The tension reaction anchors consisted of tremie-grouted 63 mm Grade 520 MPa reinforcing bars socketed more than 6.5 m into rock. The reaction beam was comprised of a heavily stiffened pair of W762 x 257 wide-flange beams strapped together for composite action and with a split-spacing of 152 mm to allow for the tension reaction members. The minimum yield strength of the test beams was 345 MPa. After setup of the loading frame, the tension reaction anchors were proof-tested to ensure that they had adequate capacity and then prestressed to 100% of their anticipated loading during the load test, equal to 890 kN each.



Figure 4. NUMA Superjaws concentric overburden drilling system

INITIAL TEST

The geotechnical specialty contractor performed a cyclic compression load test on the test pile in November 2008. The load test was conducted to a maximum load of 1,780 kN, twice the design (working) load of 890 kN, in general accordance with PennDOT specifications and ASTM D1143-07 using a quick cyclic loading sequence. Test loads were applied in typical increments of 15% of the design load, with unload-reload cycles initiated at 45%, 100%, 145%, and 200%. The load was maintained for a sixty minute period at 130% of the design load to make an examination of the time-dependent pile settlement (i.e. creep) at an elevated load level. The results of the load test were satisfactory, with measured settlements at design load and test load of 11.5 mm and 28.6 mm, respectively. Upon unloading back to zero load at the completion of the test, the permanent net settlement of the test pile was 2.5 mm, allowing that the gross load-deformation behavior to be classified as pseudo-elastic. A plot of pile top load versus settlement is presented in Figure 5. Further analysis of the load test results will be presented in later sections.

RE-TEST FOR ADDITIONAL CAPACITY

In order to provide sufficient evidence of the increased micropile Strength Limit resistance (1,690 kN) needed for economical retrofit of Pier 10N, the original test pile installed for Pier 10S was re-tested. The proposed new design (working) load was 1,280 kN, and the design consultant requested that the new compression load test be carried out to at least 200% of the working load, resulting in a new maximum test load of 2,560 kN. The geotechnical specialty contractor, who had designed the load test reaction frame, indicated to the project team that the maximum achievable test load beyond the specified level was 3,180 kN, equal to approximately 250% of the working load. This load level represented an elevated safe tension limit for the 63 mm reaction reinforcing bars corresponding to 90% of the actual material yield stress (552 MPa). Furthermore, applied loads up to this load level required allowing an overstress of 20% in bending.

Quick cyclic loading sequences were used for the re-test process. Unload-reload cycles were initiated at load levels corresponding to 45%, 100%, 145%, and 200% of the new design

(working) load. A plot of the load test data is included in Figure 6. The results of the re-test verified that the geotechnical and structural capacity and deformation characteristics were still satisfactory under the new, elevated working load of 1,280 kN. At this load level, the pile-top settlement was 18.2 mm. At the 130% load level, a 60 minute maintained load period was monitored to check for creep with less than 0.05 mm of creep movement recorded. At the required maximum test load of 2,560 kN, the vertical deflection was 40.8 mm. After unloading back to an alignment load, the micropile was then monotonically re-loaded up to 3,180 kN, with a maximum measured settlement of 54.2 mm. A net permanent settlement measurement was not made during the final loading cycle up to 3,180 kN, but the permanent settlement after reaching the required maximum test load of 2,560 kN was only 2 mm.

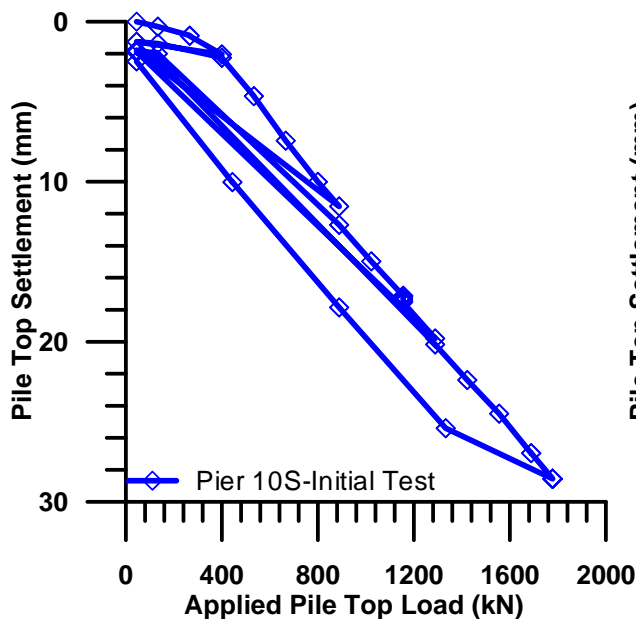


Figure 5. Load-settlement data for initial loading of test pile

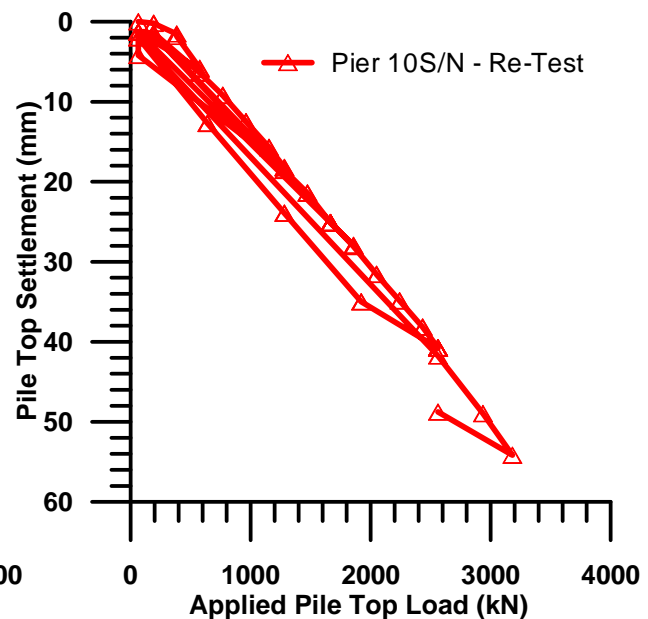


Figure 6. Load-settlement data for re-loading of test pile

MICROPILE CONSTRUCTION FOR PIER 10S AND PIER 10N

Construction of the thirty three production micropiles involved working within a narrow area while using full-size hydraulic drilling rigs, as shown in Figure 7. While test pile construction and load testing was occurring, the general contractor completed demolition of the Pier 10S substructure and crash wall. The crash wall was demolished down to existing grade leaving only 1.2 m remaining and allowing the specialty contractor full access to the 4.9 m wide work area to begin installation of micropile casings down to the top of the competent rock surface. Conventional air-powered down the hole hammers were used to penetrate from existing grade to the bottom of the existing reinforced concrete pile cap. This drilling system was preferred to penetrate through the moderately reinforced pile cap over a rotary concrete coring system for speed and economy. The presence of a single layer of reinforcement at the bottom of the existing pier pile cap made percussion drilling feasible and ultimately successful. After advancing the 194 mm OD casing through the existing pile cap and crash wall, the inner drill string was switched over to a concentric overburden system to advance down the top of competent rock. Compressed air was the drilling medium used to move drill cuttings to the surface, with water added during the process for dust suppression. The overburden drilling

system used for this project and matched up to the selected casing size has two wing bits whose expanded diameter was 197 mm. The design consultant had requested that if an overburden drilling system were used that the size be selected to limit the annulus around a micropile and reduce the potential for increased lateral deflection. Furthermore, the use of a drilling system sized to minimize overcut around the casing would provide a tighter seal in the competent rock, lessening the chances of grout loss. The selected drilling system easily penetrated through the soft, broken claystone layers that had caused the problems with the original foundation's capacity.



Figure 7. Casagrande M9-1 hydraulic drilling rig operating within 4.9 wide area at Pier 10S

After successful completion of the load test at Pier 10S, the rock sockets were constructed to the same length and diameter as the test pile, followed by installation of the 63 mm reinforcing bars and tremie grouting of the entire pile. All thirty three micropiles used to re-support Pier 10S were installed in this manner, with an average total pile length of 25.6 m. The micropiles at Pier 10N were installed immediately following those at Pier 10S and the results of the pile re-test. The observed depth to competent bedrock was similar, and the final pile lengths were ultimately very near to those at Pier 10S. The planned total of twenty two micropiles was installed at Pier 10N.

Retrofitting of existing structures with micropiles requires special consideration of how to make connections and transfer loads. Due to the substructure damage at Pier 10S and the temporary support of the spans above on shoring towers, the connection of the thirty three micropiles to the new pile cap was simplified. Without tension loads on the piles, a conventional compression connection consisting of a locked-down heavy bearing plate was used. Figure 8 depicts the Pier 10S micropiles just prior to placement of reinforcement and new concrete for the pile cap. The bearing plate on top of each vertical pile consisted of a 228.6 mm square, 41.3 mm thick

plate. Once the new pile cap, columns, and pier cap were constructed, the superstructure loads were transferred directly to the new pile group.

The retrofit of Pier 10N depended on making the micropiles integral with a partial pile cap and the existing crash wall, transferring the full loads from the superstructure above. The design consultant initially considered conventional shear dowels, but the installation of nearly 480 mild steel bars would have compromised the integrity of the existing crash wall. In addition, this sort of connection does not provide a high degree of rigidity to the new composite foundation, allowing displacements and degradation patterns not typical of new, complete pile caps. The potential for an open construction joint may have permitted intrusion of moisture, leading to premature degradation. To counteract this situation, the design consultant proposed to use Gr. 1035 post tensioning bars to enhance the shear transfer to the crash wall as shown in Figure 9. The cost of installing larger post-tensioning bars was slightly less than the cost of the mild steel bars, but this solution was thought to provide greater long term serviceability.



Figure 8. Cutoff micropiles with pile-top connections installed at Pier 10S

PSEUDO-ELASTIC ANALYSIS OF LOAD TESTS

Cyclic compression load tests such as those conducted for this project provide multiple opportunities for assessing micropile performance. The cyclic nature of the load tests, similar to performance tests of ground anchors (tiebacks) specified in Post Tensioning Institute (2004) Recommendations for Prestressed Rock and Soil Anchors, allows for the separation of pseudo-elastic and irrecoverable deformations. Pseudo-elastic elastic stiffness and permanent deformation of the micropile can be analyzed as a function of load level. Further analysis permits a simplified assessment of load transfer between pile and ground and the development of residual load as a function of load cycling. Portions of these analyses for the Birmingham Bridge load tests were presented in Holman (2009) as part of a larger compilation of test data related to the stiffness of micropile foundations in soil and rock.

The axial stiffness of any deep foundation is frequently of interest to any analyst wishing to predict performance of a structure under axial compression or tension loading. Typical analyses by structural engineers will require knowledge of the elastic stiffness k , commonly assumed to represent the deflection-load response of an elastic spring in accordance with the relationship $P=Kx$, where P is the applied load, x is the resulting displacement, and K is the spring constant. The reciprocal of K is called k , and is assumed to be a spring stiffness, more correctly referred to as a spring compliance. It is frequently assumed in structural analysis that up to design or working load-carrying capacity, a deep foundation's response is elastic. The spring response of a micropile, assumed to be a constant value for a given pile and load level, can be assessed from the results of static or cyclic compression load tests. More detailed analysis of load-deflection data from a compression or tension load test allows for an assessment of the spring constant k , which can be related to the modulus of elasticity E_p for the micropile with assumptions of linear elasticity. However, it is a misconception to assume that there is any one single elastic spring constant. In fact, k can be determined such that it contains inelastic soil and micropile response, or such that it represents the elastic soil and micropile response.



Figure 9. Post-tensioned pile cap (adapted from Splitstone et al, 2010)

Elastic Spring Compliance

Cyclic compression tests, conducted in accordance with loading schedules detailed in Sabatini et al (2005) and as adapted from tieback performance testing as recommended by the Post Tensioning Institute (2004), are often executed for micropile projects. These tests frequently consist of multiple unload-reload cycles with each cycle being longer than the previous to progressively load the pile, and then examine the residual or permanent settlement corresponding to the previous maximum load. Typical loading cycles are in increments of 25% of the working or design compression load with maximum loads of 200% to 250% of the design load. Shorter load increments were used in this project, but with only 4 to 5 load cycles.

The cyclic loading and unloading deformation data were decomposed into elastic and residual deformations allows for more advanced interpretation of the pseudo-elastic behavior of the micropiles. At the end of each loading cycle, the total pile settlement is δ_t . Upon unloading back to zero or near zero load, the measured permanent or residual settlement is δ_r . The elastic portion of the settlement δ_e corresponding to that load cycle is then calculated as

$$\delta_e = \delta_t - \delta_r \quad (\text{Eq. 4})$$

Understanding that the micropile deflection data can be separated into its elastic or recoverable and residual or irrecoverable components provides the pseudo-elastic response under the action of increasing compression load. Figure 10 presents the elastic and residual response curves for the two tests conducted for this project. From each graph it is apparent that the elastic responses contain linear portions within the range of loading to which the piles were subjected. Some slight curvature can be observed in the data sets. Linear regression of the elastic data results in slopes of $k=1.85$ to 1.74×10^{-2} mm/kN, representing the elastic compliance of the micropile. The initial loading cycle appears to have a greater elastic compliance than the re-tested pile, perhaps because of the effects of repeated load cycles on the development of residual loads within the micropile, resulting in “stiffer” loading behavior during the second and subsequent loading cycles. This is contrary to the typical behavior of cyclically loaded deep foundations in soils where hysteretic degradation effect occurs and repeated cycling causes softening of the pile response. Once the number of cycles increases to a significant number (5 or more), Gomez et al (2003) predicts that debonding effects will occur as the rock interface softens, resulting in a decreased stiffness and increased compliance. A slight degree of curvature can be detected for both elastic cycles, but the maximum loading, far from a structural or geotechnical failure, did not allow for any reliable nonlinear trend to be detected. The residual portion of each plot is curvilinear and the residual displacements δ_r are very small, indicating that the majority of the pile’s response is elastic in nature. Again, the re-tested pile demonstrated smaller values of residual displacement than the initial test except as the previous maximum test load was approached and exceeded. Increasing incremental residual displacements, indicating debonding of the rock socket, were observed at the end of the re-test when the pipe-top load exceeded 2,500 kN. The slope of the elastic data is significant in that it is believed to contain the real pseudo-elastic load-deformation behavior for these micropiles in a certain range of loading.

The elastic spring compliance k_e is a significant mechanical feature of the micropile response that can be tied to an indicator of the axial stiffness, $E_p A_p$, and mobilization of geotechnical resistance along the micropiles’ length. For an elastic bar or column under tension or compression loading, the estimated deflection δ_e is:

$$\delta_e = \frac{PL_e}{EA} \quad (\text{Eq. 5})$$

where P is the applied load, L_e is the effective elastic length, and the term EA is the axial stiffness. By rearranging terms to create the expression to describe the elastic spring compliance k_e :

$$k_e = \frac{\delta_e}{P} = \frac{L_e}{E_p A_p} \quad (\text{Eq. 6})$$

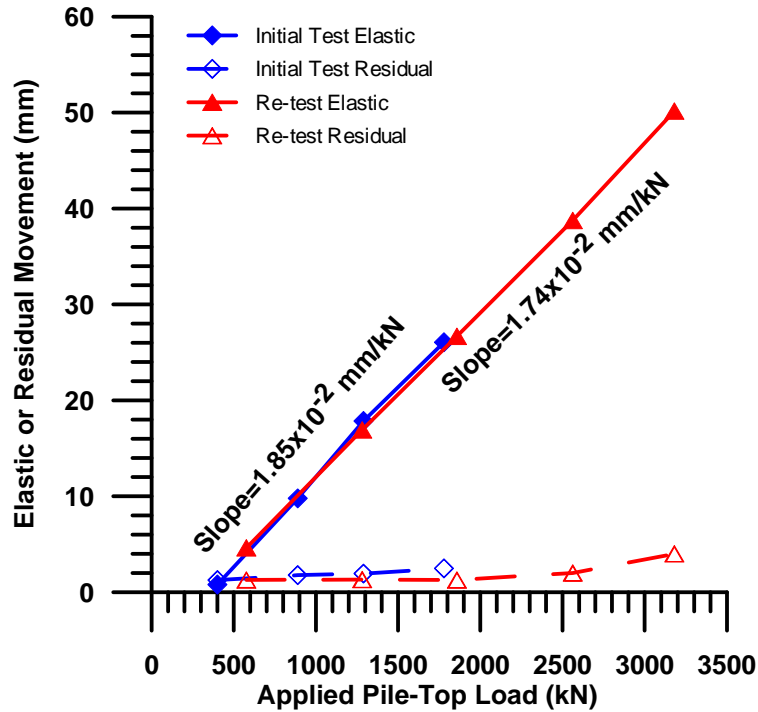


Figure 10. Decomposed cyclic loading and unloading data from Birmingham Bridge initial test and re-test

From Eq. 5 the link between spring stiffness and modulus can be seen, but there are complicating factors in directly using k_e to approximate E_p . First, the elastic response obtained by analyzing cyclic compression tests to obtain k_e contains the whole-pile behavior. However, the micropile is composite with separate $E_p A_p$ for the cased length and bond length. So, in this regard, the denominator is not a constant, single value for a uniform cross section pile. In addition, it has already been demonstrated that the elastic modulus of a micropile is not a constant value but decreases as a function of strain level with different initial tangent modulus and degradation rate for the cased and bond zone (Holman, 2009). The effective elastic length L_e is intended to be the length of pile that is debonded and acting as a free column which can shorten or extend in an unrestricted manner. Bruce and Juran (1997) refer to this as the “partially bonded” micropile and assume that until there is load transfer and progressive debonding in the bond length or rock socket. Bruce and Juran (1997), Gomez et al (2003), and Bruce et al (1993) refer to k_e as the Elastic Ratio (ER). The partially bonded concept and the validity of k_e as the elastic spring stiffness also presume that there is no residual load built up in the micropile following UR cycles. This presumption goes to simplify analysis of load test results using this manner but with the exception of piles with short cased length through very weak overburden soils, incomplete unload-reload processes and the corresponding residual loads are a fact for even monotonically loaded micropiles (Richards, 2005).

Apparent Elastic Length

The factors described above notwithstanding, the elastic compliance concept for a micropile can be used in the generation of apparent elastic length L_e and estimation of load transfer. Apparent elastic length L_e is a calculated quantity for micropiles in tension and compression and denotes the portion of the pile that is able to undergo elastic (recoverable) shortening equal to that of a freestanding column under the same load. The apparent elastic length concept

assumes that the axial stiffness $E_p A_p$ is a constant along the length of the micropile and at all load levels. For micropiles with long cased lengths where there is likely to be significant side resistance generated between casing and the surrounding ground, the cased length is not immediately free to compress freely under compression load; load must be shed to the ground prior to load transfer occurring in the bond zone or rock socket. While research and instrumented case histories have shown conclusively that linear elasticity is not applicable for micropiles or other composite deep foundations composed of steel and cementitious materials (Fellenius 1989; Holman, 2009), in the interest of maintaining simplicity for analysis, $E_p A_p$ will be calculated using assumed confined grout moduli and assuming that there is no strain-degradaton. The apparent elastic length L_e is calculated as

$$L_e = \frac{\delta_e E_p A_p}{P_n} \quad (\text{Eq. 7})$$

where P_n is the net applied compression load, defined as the total load P_t minus the alignment load P_{align} (if applied). For the analysis of this project data, the apparent elastic length is calculated as the sum of the mobilized elastic lengths of the cased length and rock socket, with different $E_p A_p$ applied for each to reflect the difference in mechanical performance of the composite micropile. By analyzing the cased and bond lengths of the micropiles separately for long piles such as these, the inevitable load transfer between casing and surrounding overburden can be explicitly included. By assuming a constant grout modulus of 1.72 GPa, the nonlinear development of L_e with increasing pile-top load can be observed for the initial test and re-test as shown in Figure 11. The computed values of the axial stiffness $E_p A_p$ for the cased length and rock socket were taken as 1,653 MN and 1,138 MN, respectively, with E_p calculated for each pile segment assuming elastic superposition of steel and grout contributions as a function of their respective cross sectional areas.

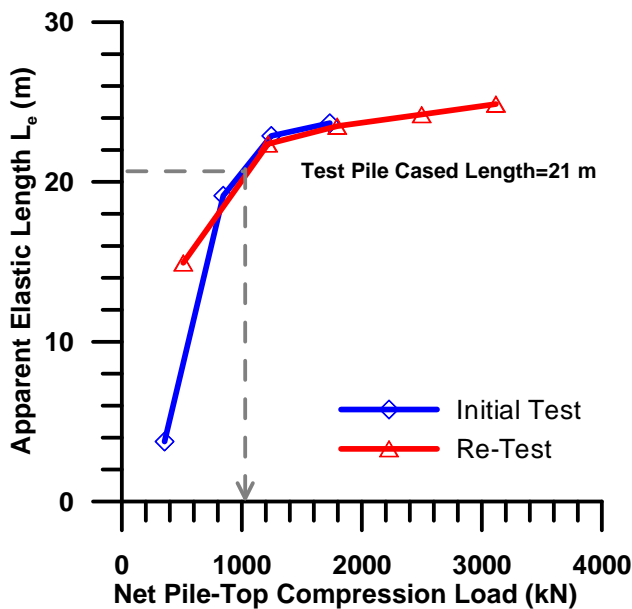


Figure 11. Development of total apparent elastic length L_e

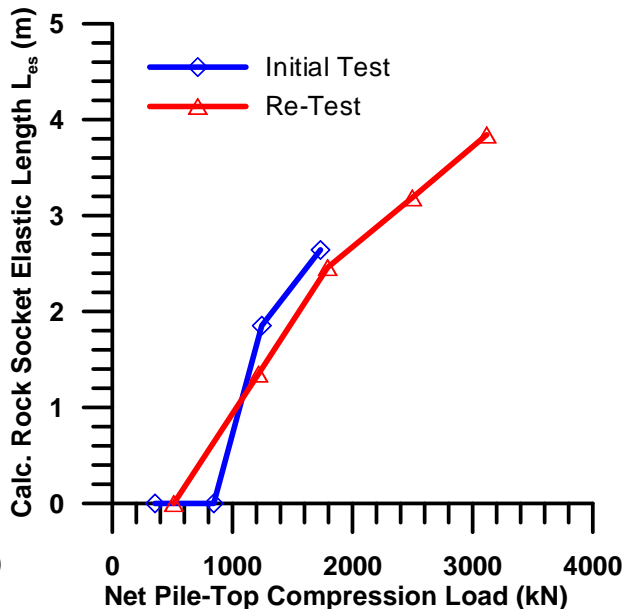


Figure 12. Development of apparent elastic length L_{er} in the rock socket

The development of the apparent elastic length is nonlinear as a function of applied pile-top load. From the calculated response of the pile presented in Figure 11, the transition between load transfer from the cased length to overburden and the initial development of load transfer in the rock socket can be seen to occur in the vicinity of an applied load of 1 MN. This is a significant load magnitude considering the frequent and near impossible assumption that no load is shed between casing and the overburden soils. For this project, where the outside diameter of the overburden drilling system is essentially the same as the casing diameter, 194 to 197 mm, there would be significant contact area between soils and weak rock and the casing exterior. As an extension of the overall elastic length concept, the rock socket's apparent elastic length was determined and plotted versus the pile-top load for both testing cycles. Referring to Figure 12, three important observations can be made: the rock socket load transfer is nonlinear, there are behavioral differences in the initial versus re-test loading, and it appears that there may have been some load development toward the bottom of the rock socket at the maximum sustained load of 3.18 MN. The estimated load transfer in the cased length and rock socket will be discussed below in further detail. Gomez et al (2003) found in cyclically loading a rock-socketed micropile that with added hysteretic loading the apparent elastic length appeared to increase, with significant increases appearing after 5 cycles. The computed elastic length in the rock socket at the conclusion of the test approached 4 m, close to the bottom of the test pile's rock socket. While the apparent elastic length concept cannot predict the actual development of end-bearing conditions, it can signal that an elastic interaction front between pile and the rock mass is approaching the rock mass beneath the pile tip.

Interpretation of apparent elastic length data and calculations is subjective without the use of strain gauge instrumentation or extensive tell-tale data to corroborate. Gomez et al (2007) indicates that the apparent elastic length of a micropile bond zone in soil is twice that obtained by the simplified calculation process. Richards (2005) indicates similar differences. Neither of these two references indicates why there is a factor of two between the calculated and what is believed to be the real elastic length. Strict interpretation of elastic length must be related to the assumed load transfer distribution. For a uniform bond distribution in prestressed ground anchors loaded in tension, as assumed and described in PTI (2004), the total depth of load transfer is twice the apparent elastic length within the bond zone. Micropiles and other deep foundations loaded in compression do not necessarily follow this simplified model. Nonlinear load transfer is commonly seen to result in parabolic or nth degree semisegment or spandrel shaped transfer diagrams, as frequently observed in strain gauge instrumented deep foundations. For real behavior observed in the field, it is possible that the apparent elastic length represents a geometric centroid of the load transfer diagram.

Load Transfer

For analysis of the cyclic compression load test data, the calculated L_e values for the cased length and rock socket were used to assess the gross load transfer to the overburden soils, weak rock, and competent rock. The cased length and rock socket were considered separately using the data generated in Figures 11 and 12. Each load cycle can be used to assess the mobilized uniform bond stress within the rock socket, followed by an assessment of the overall load distribution diagram from the plot of elastic length versus load.

It is notable that from the interpretation of the elastic length data, the cased portion of the pile contributed a significant portion of the the overall micropile capacity, but that the calculated contribution is larger for initial loading than for the re-test. During initial loading, L_e did not approach the actual cased length of the test pile until a net load of 844 kN was applied. From

this piece of information, and the “soft” nature of the load versus effective length relationship in Figure 11, it can be presumed that the load began to transfer to the top of the rock socket near or after this pile-top load. An average load transfer rate from the pile casing to the overburden soils and weak rock can be estimated as 44 kN/m, equating to a mobilized uniform bond shear stress τ_{mob} of 72 kPa. This may not represent a true ultimate bond stress τ_{ult} because the overall deflection near the top of the rock socket is not sufficient to permit the entire cased length to experience relative pile to soil movement needed to develop interface failure conditions. It is notable that, contrary to assumptions made to simplify load test data, there is real, measurable load transfer from cased length to the surrounding ground. In the case of this project, the calculated load transfer is nearly enough to sustain the entire pile design (working) axial load or Strength Limit load.

The mobilization of load transfer in the rock socket occurs as a function of complex interaction between the heavily reinforced grout bond length and the variable nature of the intact rock mass below the weak, broken claystone. Interface mechanics between the rock mass and grout under load are very complex because of the dependence of bond shear stress on the ratio of pile to rock mass deformation moduli, dilation as a function of socket compression and generation of high normal stresses, and time, among other factors. For this series of cyclic load tests, the transfer of load from the rock socket to the surrounding rock mass can be assessed using the relationships plotted in Figure 13, which are the curves from Figure 12 zeroed out to reflect only the load increments affecting the rock socket. Table 3 summarizes the average bond stresses calculated from the apparent elastic lengths for the rock socket. The calculated data presented in Table 3 describe the evolution of bond shear resistance in the rock socket with each cycle of load after the elastic length of the micropile exceeds the simple cased length. For the initial loading, it can be seen that shear resistance is generated in the rock socket, primarily as a result of the fact that the cased portion of the pile withstands a great portion of the test load. For the re-loading of the test pile, the calculated average bond stresses progressively increase with added load at the socket top. These calculated bond stresses have not been corrected for any effects of load distribution type or shape. Application of a factor of two, as recommended and discussed previously, would reduce the calculated τ_{mob} by precisely one-half. In addition, if the suggested multiplier on L_e were applied, the resulting calculated lengths would be greater than the actual rock socket length, suggesting that load was being dissipated beneath the pile tip in end-bearing. While this is not impossible, it is highly unlikely for micropiles in competent rock at loads significantly less than failure, which can be evidenced by the fact that the residual displacements are still low even at loads approaching 3.2 MN.

The patterns of load transfer revealed in this pseudo-elastic analysis, in Figure 13 and Table 3 demonstrate that a transition in socket behavior occurs during the loading process. For the initial load test, load begins to develop in the rock socket beyond a net pile-top load of about 850 kN, with a transition in apparent load transfer occurring at a total test load of 1,244 kN. Based on the calculated socket elastic length of 2.64 at the conclusion of the initial test, the increase in load transfer is meaningful because it corresponds to the beginning of the micropile interaction with the stiffer, higher RQD rock near and below Elev. 202. On reloading the micropile for the subsequent re-test, the load rapidly transfers through the overburden to the rock socket, followed by a transition to a stiffer response at a pile top load of about 1,800 kN, very similar to the maximum test load of the original test. The elastic length to which this load level corresponds indicates the mobilized bond length is in or very near to the more competent, unweathered sandy siltstone making up the lower portion of the rock socket. Based on these observations, it can be seen that graphical depictions of L_e in the rock socket can denote changes in load transfer rate which can be related to changes in rock mass characteristics.

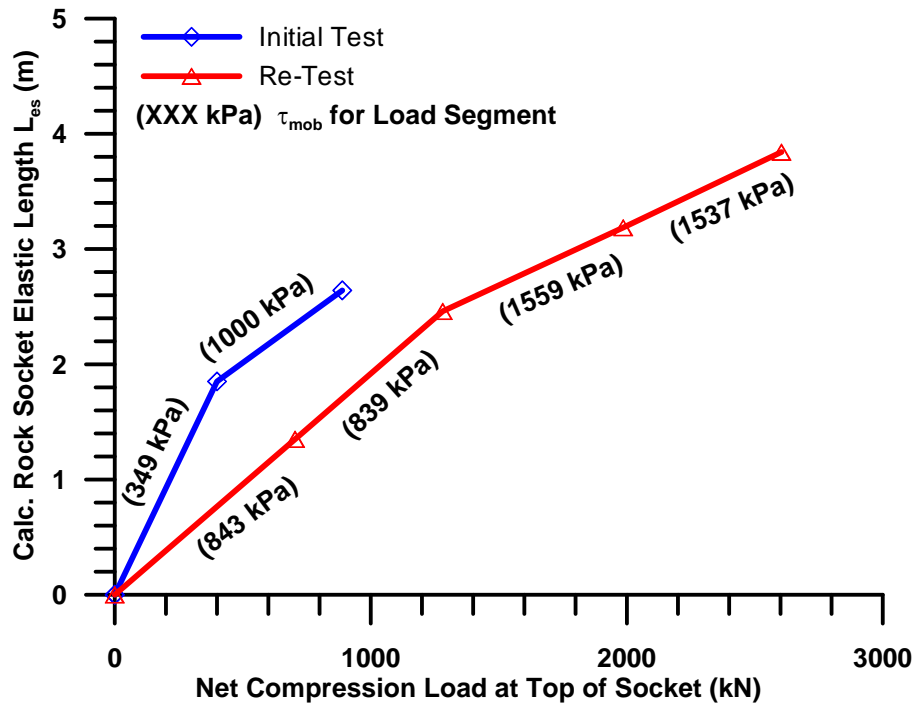


Figure 13. Incremental load transfer behavior of rock socket

Table 3. Calculated load transfer between socket and rock mass
(Note: LTR=Load Transfer Rate)

Load Cycle	Net Pile Top Load (kN)	Net Load at Top of Socket (kN)	Calc. L_{es} (m)	Calc. LTR (kN/m)	Calc. Ave. τ_{mob} (kPa)
Initial	844.3	0.0	0.00	-	-
	1244.3	399.9	1.85	216	349
	1733.1	888.8	2.64	336	543
Re-Test	512.4	0.0	0.00	-	-
	1217.0	704.6	1.35	522	843
	1793.5	1281.1	2.46	521	841
	2498.1	1985.7	3.19	623	1007
	3116.4	2604.0	3.84	678	1095

CONCLUSIONS

The Birmingham Bridge emergency repair project was a great success due to a number of factors. The first contributing factor was PennDOT's willingness to involve the geotechnical specialty contractor in the process of developing constructible solutions and a final design. A second reason was that micropiles were selected where the tooling and construction techniques offered ideal flexibility to install the piles in the given subsurface conditions. The combination of these two factors, among others, resulted in a cost effective way to reconstruct Pier 10S and stabilize Pier 10N. Drilling through the reinforced concrete of the existing pile-supported footing eliminated having to excavate and demolish the substructure which would have raised serious concerns with the stability of the bridge superstructure shoring system. Specialized down the hole hammer systems were efficient in advancing the micropile casing to the required depths through fill and overburden soils and the weak claystone bedrock. The designer's assessment that the new foundation could resist all lateral loads through vertical piles improved the constructability of this retrofit system. The use of initial load testing and re-testing of the same pile provided a relatively efficient design for Pier 10S and a more cost-effective way to retrofit Pier 10N.

Analysis of the cyclic testing data from two loads permitted a detailed examination of the development of elastic spring compliance k_e , apparent elastic length L_e , and the potential distribution of loads within the test pile's rock socket. The decomposition of total movements and rebound for each load cycle into elastic and residual displacements showed that the elastic spring compliance was similar for all ranges of load applied to the pile, with slight decrease in interpreted compliance (increased stiffness) upon reloading during the re-test. A limited increase in residual displacement was observed at the conclusion of the re-test where the loading was applied to 3,180 kN, the maximum limit of the reaction frame. Use of the apparent length concept with separate consideration of the cased length and rock socket axial stiffness $E_p A_p$ demonstrated that a significant amount of total load was transferred between the casing and overburden soils, nearly 1,000 kN, prior to mobilization of load capacity in the rock socket. Beyond this load level, bond shear stresses began to mobilize within the rock socket, with increasing pile-top load translating to increased apparent elastic length. The final shape of the load-elastic length plot indicates that a transition in socket behavior occurred around a pile-top load of 1,800 kN, where the overall average bond shear stress in the rock socket approached 1,100 kPa. This pre-failure value is comparable to safe working levels reported in the literature for similar geologic materials. The overall load-unload behavior of the micropile under both load tests indicated that no failure condition or significant debonding of the grout-rock interface was occurring, safely substantiating the higher load carrying capacity desired for Pier 10N.

ACKNOWLEDGEMENTS

The General Contractor for this project was Trumbull Corporation and their design consultant was HDR Engineering, Inc. The authors share their gratitude with these two firms for fostering constructive dialogue which lead to a very cost-effective solution to PennDOT's significant problem. Many thanks go to Moretrench field engineering and skilled labor personnel for their efforts in constructing these micropiles and conducting the load tests with great professional skill and care. The authors also wish to thank the executive management of Moretrench for supporting internal research and development efforts for the purpose of advancing the state of the art in micropile analysis and understanding.

REFERENCES

- ACI 318-05 (2005). *Building Code Requirements for Structural Concrete and Commentary, an ACI Standard*. American Concrete Institute, Committee 318, Farmington Hills, 430 pp.
- Bruce, D.A., and Juran, I. (1997). *Drilled and Grouted Micropiles: State of Practice Review, Volume II-Design*. Federal Highway Administration Report RD-96-017, 236 pp.
- Bruce, D.A., Bjorhovde, R., and Kenny, J.R. (1993). "Fundamental tests on the performance of high capacity pin piles." *Proceedings of the DFI Annual Member's Conference and Meeting*, Pittsburgh, PA, 33 pp.
- Fellenius, B. (2001). "From strain measurements to load in an instrumented pile." *Geotechnical New Magazine*, Vol. 19, No. 1, 35-38.
- Fellenius, B. (1989). "Tangent modulus of piles determined from strain data." *Proc. of the Congress on Foundation Engineering: Current Principles and Practices*, ASCE, Vol. 1, 500-510.
- Gómez, J.E., A.W. Cadden, and D.A. Bruce. (2003). "Micropiles founded in rock. Development and evolution of bond stresses under repeated loading." *Soil and Rock America 2003, Proceedings of the 12th PanAmerican Conference on Soil Mechanics and Geotechnical Engineering*, Cambridge, MA, June 22-26, pp. 1911-1916.
- Gomez, J.E., Rodriguez, C.J., Robinson, H.D., Mikitka, J., and Keough, L. (2007). "Hollow core bar micropiles – Installation, testing, and interpretation of design parameters of 260 micropiles." *Proceedings of the 8th International Workshop on Micropiles*, Toronto, Canada, 21 pp.
- Hanna, T.H. (1982). *Foundations in Tension, Ground Anchors*. Trans-Tech Publications and McGraw-Hill Book Company, First Edition. 573 pp.
- Holman, T.P. (2009). "Pseudo-elastic performance and response of micropiles." *Proceedings of the 9th International Workshop on Micropiles*, London, United Kingdom, May 10-13, 19 pp.
- Olson, L.D., Jalinoos, F., and Aouad, M.F. (1998). *Summary of the NCHRP 21-5 Interim Report, Determination of Unknown Subsurface Bridge Foundations, Geotechnical Engineering Notebook Issuance GT-16*, Federal Highway Administration, 71 pp.
- PTI (2004). *Recommendations for Prestressed Rock and Soil Anchors*. Post Tensioning Institute, 98 pp.
- Richards, T. (2005). "Pent-up load and its effect on load test evaluation." *Proc. of the GEO Construction Quality Assurance/Quality Control Technical Conference*, ADSC: The International Association of Foundation Drilling, 127-134.
- Sabatini, P.J., Tanyu, B., Armour, T., Groneck, P. and Keeley J.W. (2005). *Micropile Design and Construction Reference Manual*. Federal Highway Administration Report NHI-05-039, 456 pp.
- Splitstone, D.E., Stonecheck, S.A., Dodson, R.L., and Fuller, J.A. (2010). "Birmingham Bridge Emergency Repairs: Micropile Foundation Retrofit," *Proceedings of GeoFlorida 2010: Advances in Analysis, Modeling, and Design*, Fratta et al, eds., ASCE Geotechnical Special Publication No. 199, 9 pp.